Optical polarimetric study of open clusters: distribution of interstellar matter towards NGC 654

Biman J. Medhi,[1]★ Maheswar G., [1,2] J. C. Pandey,[1] T. S. Kumar[1] and Ram Sagar[1]

[1]*Aryabhatta Research Institute of Observational Sciences, Manora Peak, Nainital 263129, India*
[2]*Korea Astronomy and Space Science Institute 61-1, Hwaam-dong, Yuseong-gu, Daejeon 305-348, Korea*

ABSTRACT

We present new B, V and R linear polarimetric observations for 61 stars towards the region of the young open cluster NGC 654. In this study we found evidence for the presence of at least two layers of dust along the line of sight to the cluster. The distances to the two dust layers are estimated to be $\sim$200 pc and $\sim$1 kpc which are located much closer to the Sun than the cluster ($\sim$2.4 kpc). Both the dust layers have their local magnetic field orientation nearly parallel to the direction of the Galactic plane. The foreground dust layer is found to have a ring morphology with the central hole coinciding with the centre of the cluster. The foreground dust grains are suggested to be mainly responsible for both the observed differential reddening and the polarization towards the cluster.

Key words: polarization – dust, extinction – open clusters and associations: individual: NGC 654.

1 INTRODUCTION

The wavelength dependence of interstellar extinction and polarization provides constraints on the characteristics of interstellar grains. Interstellar polarization strongly varies with wavelength (Serkowski, Mathewson & Ford 1975; Wilking et al. 1980). In particular, the wavelength of maximum interstellar polarization (λ_{max}) is thought to be related to the total-to-selective extinction (R_V) as $R_V = (5.6 \pm 0.3)\lambda_{max}$ (Whittet & van Breda 1978). The polarization of background starlight has been used for nearly five decades to probe the magnetic field direction in the interstellar medium (ISM). The observed polarization is believed to be caused by the dichroic extinction of background starlight passing through the concentrations of aligned and elongated dust grains along the line of sight. Although there is no general consensus on which is the dominant grain alignment mechanism (Lazarian, Goodman & Myers 1997), it is generally believed that the elongated grains tend to become aligned to the local magnetic field with their shortest axis parallel to the field. For this orientation, the observed polarization vector is parallel to the plane-of-sky projection of a line-of-sight averaged magnetic field (Davis & Greenstein 1951).

Young open clusters are very good candidates to carry out the polarimetric observations because of the available knowledge on their physical parameters such as distance, membership probability (M_P) and colour excess [$E(B - V)$]. This would enable us to undertake a meaningful study of foreground interstellar dust.

As a part of an observational programme to carry out polarimetric observations of young open clusters towards antigalactic centre direction ($l = 120°$–$180°$) to investigate the properties like magnetic field orientation, λ_{max}, maximum polarization (P_{max}), etc., we observed two young open cluster IC 1805 (Medhi et al. 2007) and NGC 654. In this paper we present the results obtained from our study on NGC 654. The young open cluster NGC 654(RA (J2000) $01^h44^m00^s$, Dec.(J2000) $+61°53'06''$; $l = 129°.08$, $b = -00°.36$) in Cassiopeia has been classified as Trumpler class II2r by Lyngå (1984). The post-main-sequence stars in NGC 654 reveal an age of $\sim$10–30 Myr for the cluster, whereas the pre-main-sequence stars indicate an age of $\sim$1–10 Myr (Pandey et al. 2005). The value of $E(B - V)$ across the cluster varies in the range $\sim$0.7–1.2 mag (Joshi & Sagar 1983; Phelps & Janes 1994). A distance modulus of 14.7 ± 0.10, which corresponds to 2.41 ± 0.11 kpc (for a normal reddening law), is estimated for the cluster (Pandey et al. 2005).

First polarimetric measurements of the stars towards NGC 654 were made by Samson (1976) with plates using IIa0 emulsion (IIa0 emulsion has a red cut-off similar to Johnson B band). Samson (1976) found certain stars to be very conspicuous because they differed in magnitude or direction of polarization, or both, from the surrounding stars. Star #37, for example, was unusual in both the magnitude and direction of polarization. He suggested a dust cloud partially obscuring the area to be the reason. The general direction of polarization was found to be parallel to the Galactic magnetic field. Recently, Pandey et al. (2005) observed seven stars in the vicinity of NGC 654. Of these seven stars, four of them with higher membership probability (M_P) showed relatively large polarization (3.03–4.47 per cent) and a mean position angle PA $_V \simeq 94°$ in V filter.

★E-mail: biman@aries.ernet.in

The two non-member stars showed relatively small polarization ($\sim$2 per cent) and a mean PA $_V \simeq 105°$. The remaining star #57 with $M_P = 0.90$ (Stone 1977) was identified as a non-member (Sagar & Yu 1989) also showed values (2 per cent and 102°) similar to those of two non-member stars. From their multiwavelength study, they concluded that the dust grains associated with NGC 654 are smaller than those associated with the general ISM.

In this paper, we present the results of polarimetric measurements made for 61 stars in B, V and R photometric bands towards NGC 654 (brighter than $V \simeq 17$ mag). Of the 61 stars observed, eight of them have high membership probability ($M_P \geq 0.7$). The paper is organized as following: in Section 2 we present observations; the results and discussion are presented in Section 3 and in Section 4 we conclude with a summary.

2 OBSERVATIONS

The optical imaging polarimetric observations of the two fields (centred at RA $01^h43^m19^s$, Dec. $+61°51'31''$ and RA $01^h43^m56^s$, Dec. $+61°57'48''$) in NGC 654 were carried out on 2006 December 27 and 28 using ARIES Imaging Polarimeter (AIMPOL; Rautela, Joshi & Pandey 2004; Medhi et al. 2007) mounted on the Cassegrain focus of the 104-cm Sampurnanand telescope of ARIES, Nainital, in B, V and R ($\lambda_{B_{\rm eff}} = 0.440$ μm, $\lambda_{V_{\rm eff}} = 0.550$ μm and $\lambda_{R_{\rm eff}} = 0.660$ μm) photometric bands. The imaging was done by using a TK 1024 × 1024 pixel^2 CCD camera. Each pixel of the CCD corresponds to 1.7 arcsec and the field of view is $\sim$8 arcmin diameter on the sky. The FWHM of the stellar image varies from 2 to 3 pixel. The readout noise and gain of the CCD are 7.0 e$^-$ and 11.98 e$^-$ ADU^{-1}, respectively. The fluxes for all of our programme stars were extracted by aperture photometry after the bias subtraction in the standard manner using IRAF. The detail descriptions about the AIMPOL, data reduction and calculations of polarization and position angle are given in Medhi et al. (2007).

Standard stars for null polarization and for the zero-point of the polarization position angle were taken from Schmidt, Elston & Lupie (1992). The observed degree of polarization (P per cent) and

position angle (θ) for the polarized standard stars and their corresponding values from Schmidt et al. (1992) are given in Table 1. The observed values of P per cent and θ are in good agreement with those given in Schmidt et al. (1992) within the observational errors. The observed normalized Stokes parameters q per cent and u per cent for standard unpolarized stars (Schmidt et al. 1992) are also given in Table 1. The average value of instrumental polarization is found to be $\sim$0.04 per cent.

The ordinary and extraordinary images of each source in the CCD frame are separated by 27 pixels along the north–south direction on the sky plane. Due to the lack of a grid, placed to avoid the overlapping of ordinary image of one source with the extraordinary of an adjacent one located 27 pixels away along the north–south direction, we avoided the central crowded portion of the cluster. However, the fields are chosen in such a manner to include maximum number of member stars. We also had a large number of sources which are not members but are present in the fields observed. All the sources were manually checked and rejected in the case of an overlapping. But background at any location of the observed field gets doubled due to this overlapping and may have significant effect if the background has variation within 27 pixels (e.g. presence of reflection nebulosity). One star, BD+61 315, is found to be associated with a faint nebulosity. We suspect that, due to the lack of grid in our polarimeter, the reflection nebulosity may have contributed polarized light over the aperture used for the photometry. We discuss this issue in Section 3.

3 RESULTS AND DISCUSSION

Our polarimetric results are presented in the Table 2. Column 2 gives the star identification as given by Phelps & Janes (1994). Instrumental magnitudes obtained in V filter are given in column 3. The measured values of polarization P (in per cent) and the corresponding error ϵ (in per cent) in B, V and R filters are given in columns 4, 6 and 8, respectively. The polarization position angle (of the $\boldsymbol{E}$ vector) θ (in degrees) and the corresponding error ϵ (in degrees) in B, V and R filters are given in columns 5, 7 and 9,

Table 1. Observed polarized and unpolarized standard stars.

| Filter | Polarized standard | | | | Unpolarized standard | |
| | $P \pm \epsilon$ (per cent) | $\theta \pm \epsilon(°)$ | $P \pm \epsilon$ (per cent) | $\theta \pm \epsilon(°)$ | q (per cent) | u (per cent) |
	Schmidt et al. (1992)		This paper		This paper	
	Hiltner-960				HD21447	
B	5.72 ± 0.06	55.06 ± 0.31	5.62 ± 0.20	54.65 ± 1.04	0.019	0.011
V	5.66 ± 0.02	54.79 ± 0.11	5.70 ± 0.14	53.37 ± 0.08	0.037	-0.031
R	5.21 ± 0.03	54.54 ± 0.16	5.20 ± 0.06	54.80 ± 0.38	-0.035	-0.039
	HD 204827				HD12021	
B	5.65 ± 0.02	58.20 ± 0.11	5.72 ± 0.09	58.60 ± 0.49	-0.108	0.071
V	5.32 ± 0.02	58.73 ± 0.08	5.35 ± 0.03	60.10 ± 0.20	0.042	-0.045
R	4.89 ± 0.03	59.10 ± 0.17	4.91 ± 0.20	58.89 ± 1.20	0.020	0.031
	BD+64°106				HD14069	
B	5.51 ± 0.09	97.15 ± 0.47	5.46 ± 0.10	99.40 ± 0.50	0.138	-0.010
V	5.69 ± 0.04	96.63 ± 0.18	5.48 ± 0.11	97.09 ± 0.12	0.021	0.018
R	5.15 ± 0.10	96.74 ± 0.54	5.20 ± 0.02	97.35 ± 0.18	0.010	-0.014
	HD 19820				G191B2B	
B	4.70 ± 0.04	115.70 ± 0.22	4.81 ± 0.20	113.49 ± 0.19	0.072	-0.059
V	4.79 ± 0.03	114.93 ± 0.17	4.91 ± 0.10	114.55 ± 0.20	-0.022	-0.041
R	4.53 ± 0.03	114.46 ± 0.17	4.70 ± 0.13	113.88 ± 0.21	-0.036	0.027

Table 2. Observed *B*, *V* and *R* polarization values for different stars in NGC 654.

Serial No. (1)	ID (P) (2)	V (mag) (3)	$P_B \pm \epsilon$ (per cent) (4)	$\theta_B \pm \epsilon(°)$ (5)	$P_V \pm \epsilon$ (per cent) (6)	$\theta_V \pm \epsilon(°)$ (7)	$P_R \pm \epsilon$ (per cent) (8)	$\theta_R \pm \epsilon(°)$ (9)	$E(B-V)$ (10)	M_P (11)
01	–	16.66	3.37 ± 0.56	114 ± 5	3.42 ± 0.25	112 ± 2	3.47 ± 0.27	108 ± 2	–	–
02	–	16.16	3.23 ± 0.30	109 ± 3	3.22 ± 0.02	114 ± 2	3.20 ± 0.18	116 ± 2	–	–
03	–	15.17	1.57 ± 0.08	101 ± 2	1.59 ± 0.05	105 ± 1	1.57 ± 0.07	101 ± 4	–	–
04	–	17.05	3.18 ± 0.14	102 ± 1	3.86 ± 0.26	104 ± 2	3.35 ± 0.13	105 ± 2	–	–
05	–	16.71	4.15 ± 0.65	110 ± 5	4.41 ± 0.13	109 ± 1	4.10 ± 0.53	112 ± 4	–	–
06	–	14.96	2.73 ± 0.10	110 ± 1	2.79 ± 0.05	112 ± 1	2.49 ± 0.06	111 ± 1	–	–
07	–	17.65	3.03 ± 0.37	95 ± 4	3.26 ± 0.40	98 ± 4	3.12 ± 0.07	101 ± 2	–	–
08	–	15.99	3.28 ± 0.36	110 ± 3	3.63 ± 0.01	112 ± 1	3.49 ± 0.04	109 ± 1	–	–
09	–	16.68	3.26 ± 0.49	99 ± 4	3.38 ± 0.28	100 ± 2	3.38 ± 0.28	100 ± 2	–	–
10	–	17.35	3.31 ± 0.50	114 ± 4	3.64 ± 0.33	112 ± 3	3.79 ± 0.86	115 ± 7	–	–
11	–	16.62	4.27 ± 0.13	112 ± 1	4.64 ± 0.27	108 ± 2	4.69 ± 0.12	112 ± 1	–	–
12	703	13.11	3.71 ± 0.07	94 ± 1	3.82 ± 0.18	100 ± 2	3.41 ± 0.01	93 ± 1	0.78	0.70
13	–	14.93	4.33 ± 0.04	111 ± 1	4.43 ± 0.05	110 ± 1	4.09 ± 0.17	108 ± 1	–	–
14	–	14.74	2.49 ± 0.07	111 ± 1	2.71 ± 0.18	112 ± 2	2.39 ± 0.04	111 ± 1	–	–
15	–	16.98	3.66 ± 0.37	103 ± 4	3.90 ± 0.64	98 ± 5	3.51 ± 0.29	104 ± 2	–	–
16	–	16.96	3.41 ± 0.27	100 ± 4	3.96 ± 0.08	104 ± 1	3.52 ± 0.05	104 ± 1	–	–
17	–	16.20	2.13 ± 0.36	112 ± 5	3.00 ± 0.45	111 ± 4	2.23 ± 0.11	109 ± 2	–	–
18	–	17.28	1.95 ± 0.66	117 ± 10	2.67 ± 0.36	120 ± 2	2.25 ± 0.10	125 ± 1	–	–
19	–	15.68	2.54 ± 0.18	98 ± 2	2.49 ± 0.21	103 ± 2	2.36 ± 0.11	97 ± 2	–	–
20	–	16.08	2.55 ± 0.19	98 ± 2	2.63 ± 0.13	91 ± 1	2.47 ± 0.11	97 ± 2	–	–
21	–	16.19	3.04 ± 0.09	116 ± 1	3.47 ± 0.25	116 ± 2	3.01 ± 0.19	109 ± 2	–	–
22	–	15.71	2.91 ± 0.11	106 ± 1	3.13 ± 0.02	101 ± 1	2.98 ± 0.02	100 ± 1	–	–
23	–	15.75	2.62 ± 0.33	106 ± 4	2.72 ± 0.20	118 ± 2	2.71 ± 0.24	109 ± 3	–	–
24	–	15.86	1.45 ± 0.02	97 ± 1	1.60 ± 0.03	95 ± 1	1.33 ± 0.10	104 ± 2	–	–
25	–	16.05	3.54 ± 0.38	108 ± 3	4.08 ± 0.34	108 ± 3	3.44 ± 0.10	107 ± 1	–	–
26	–	15.54	0.75 ± 0.02	129 ± 1	0.97 ± 0.20	122 ± 6	0.79 ± 0.09	128 ± 4	–	–
27	–	15.94	3.19 ± 0.10	97 ± 1	3.32 ± 0.30	103 ± 3	3.17 ± 0.03	102 ± 1	–	–
28	–	17.33	4.26 ± 0.01	100 ± 1	4.69 ± 0.89	101 ± 5	3.90 ± 1.39	95 ± 10	–	–
29	530	16.84	2.51 ± 0.39	112 ± 4	2.53 ± 0.03	124 ± 1	2.31 ± 0.48	121 ± 7	1.02	–
30	648	15.69	3.19 ± 0.06	96 ± 1	3.38 ± 0.04	93 ± 1	3.30 ± 0.03	91 ± 1	0.91	–
31	641	16.06	4.39 ± 0.03	115 ± 1	4.68 ± 0.26	111 ± 2	4.10 ± 0.17	116 ± 1	0.92	–
32	642	16.87	2.61 ± 0.44	120 ± 5	2.79 ± 0.07	121 ± 1	2.65 ± 0.20	121 ± 3	1.00	–
33	637	17.52	4.79 ± 0.41	96 ± 2	4.73 ± 0.22	104 ± 1	4.78 ± 0.12	100 ± 1	1.16	–
34	493	13.78	1.77 ± 0.01	104 ± 1	1.87 ± 0.01	104 ± 3	1.83 ± 0.01	100 ± 1	0.50	0.00
35	555	10.74	4.10 ± 0.07	99 ± 1	4.37 ± 0.09	103 ± 1	4.12 ± 0.02	101 ± 1	0.88	0.84
36	634	16.33	3.57 ± 0.12	92 ± 1	3.84 ± 0.26	100 ± 2	3.15 ± 0.13	98 ± 1	1.82	–
37	450	12.86	4.28 ± 0.31	95 ± 2	4.55 ± 0.03	104 ± 1	4.23 ± 0.22	102 ± 1	0.64	0.55
38	439	14.53	4.13 ± 0.06	102 ± 5	4.23 ± 0.08	105 ± 1	4.17 ± 0.01	107 ± 2	1.08	0.89
39	556	12.86	4.56 ± 0.11	105 ± 1	4.55 ± 0.03	104 ± 1	4.35 ± 0.01	105 ± 1	0.69	0.90
40	–	15.67	2.23 ± 0.50	96 ± 6	2.90 ± 0.15	98 ± 2	2.48 ± 0.13	99 ± 2	–	–
41	–	15.96	2.41 ± 0.29	93 ± 3	2.08 ± 0.36	96 ± 5	2.30 ± 0.08	99 ± 1	–	–
42	–	16.53	2.65 ± 0.49	83 ± 5	2.99 ± 0.40	76 ± 3	2.43 ± 0.13	88 ± 2	–	–
43	–	16.84	1.72 ± 0.35	98 ± 6	2.40 ± 0.56	95 ± 7	2.04 ± 0.11	98 ± 2	–	–
44	–	16.38	2.35 ± 0.58	96 ± 7	2.67 ± 0.15	93 ± 3	2.54 ± 0.20	100 ± 2	–	–
45	474	14.87	1.27 ± 0.20	100 ± 5	1.09 ± 0.11	99 ± 3	1.15 ± 0.04	94 ± 1	0.93	–
46	405	16.51	2.28 ± 0.10	95 ± 1	2.30 ± 0.09	98 ± 4	1.97 ± 0.25	103 ± 4	1.08	–
47	322	15.51	3.78 ± 0.17	96 ± 2	3.89 ± 0.26	93 ± 3	3.91 ± 0.16	95 ± 2	1.03	0.86
48	267	16.72	2.76 ± 0.43	118 ± 5	2.91 ± 0.11	107 ± 1	2.62 ± 0.18	110 ± 2	1.47	–
49	–	16.19	4.14 ± 0.37	104 ± 3	3.89 ± 0.35	100 ± 1	3.83 ± 0.40	101 ± 3	–	–
50	238	14.93	4.35 ± 0.20	101 ± 1	4.25 ± 0.04	108 ± 1	4.26 ± 0.01	101 ± 1	0.77	0.03
51	187	16.20	4.48 ± 0.03	102 ± 1	4.53 ± 0.18	100 ± 1	4.44 ± 0.01	97 ± 2	0.90	–
52	150	17.26	4.57 ± 0.17	96 ± 1	4.68 ± 0.46	100 ± 3	4.40 ± 0.04	103 ± 1	0.94	0.11
53	132	15.93	3.58 ± 0.12	101 ± 1	3.09 ± 0.48	102 ± 4	3.50 ± 0.09	97 ± 1	0.88	–
54	119	17.39	3.44 ± 0.61	104 ± 5	3.56 ± 0.62	97 ± 5	3.57 ± 0.15	94 ± 1	0.97	0.95
55	080	17.18	5.45 ± 0.45	97 ± 11	5.10 ± 0.15	102 ± 2	4.80 ± 0.10	92 ± 2	0.80	0.11
56	–	16.80	4.10 ± 0.69	99 ± 5	4.47 ± 1.08	101 ± 12	4.01 ± 0.31	102 ± 2	–	–
57	061	16.63	3.23 ± 0.46	101 ± 15	3.55 ± 0.29	96 ± 1	3.46 ± 0.47	95 ± 4	1.11	0.83
58	034	16.75	4.61 ± 0.61	96 ± 3	4.80 ± 0.17	100 ± 1	4.53 ± 0.10	99 ± 1	0.95	0.90
59	–	15.74	4.54 ± 0.46	94 ± 3	4.04 ± 0.24	93 ± 2	4.12 ± 0.15	92 ± 1	–	–
60	562	14.70	4.21 ± 0.20	92 ± 1	4.21 ± 0.03	93 ± 1	4.12 ± 0.15	92 ± 1	1.32	–
61	563	15.60	4.12 ± 0.55	96 ± 1	3.64 ± 0.34	96 ± 3	3.72 ± 0.07	93 ± 1	0.85	–

Table 3. Results of previous polarization measurements carried out by Samson (1976) and Pandey et al. (2005) in the direction of NGC 654. The errors in the measurements are given in parentheses.

| ID	P_B (per cent)	θ_B (°)	P_V (per cent)	θ_V (°)	P_R (per cent)	θ_R (°)	P_I (per cent)	θ_I (°)	M_P (per cent)
(1)	(2)	(3)	(4)	(5)	(6)	(7)	(8)	(9)	(10)
				Samson (1976)					
1	2.12 (1.0)	88	–	–	–	–	–	–	0.86
5	6.45 (2.8)	106	–	–	–	–	–	–	0.92
8	6.95 (4.7)	136	–	–	–	–	–	–	0.92
9	6.40 (2.3)	97	–	–	–	–	–	–	0.91
14	5.80 (2.9)	92	–	–	–	–	–	–	0.82
36	5.16 (1.0)	98	–	–	–	–	–	–	0.90
37	8.52 (0.4)	141	–	–	–	–	–	–	0.92
40	12.39 (5.3)	47	–	–	–	–	–	–	0.87
41	9.03 (1.2)	95	–	–	–	–	–	–	0.82
54	7.97 (3.1)	90	–	–	–	–	–	–	0.93
56	5.48 (1.7)	80	–	–	–	–	–	–	0.00
64	4.37 (1.7)	99	–	–	–	–	–	–	0.84
65	4.88 (2.0)	88	–	–	–	–	–	–	0.89
66	13.82 (0.5)	75	–	–	–	–	–	–	0.90
				Pandey et al. (2005)					
9	2.00(0.47)	98(7)	3.03(0.16)	92(2)	2.68(0.11)	94(1)	2.31(0.17)	98(2)	0.92
57	2.16(0.36)	97(5)	2.03(0.15)	102(2)	1.48(0.14)	98(3)	1.25(0.26)	97(5)	0.90
68	4.18(0.70)	85(5)	4.47(0.19)	95(1)	3.78(0.11)	94(1)	3.42(0.18)	95(2)	0.84
109	3.86(0.22)	92(2)	3.82(0.06)	96(1)	3.23(0.05)	96(1)	3.00(0.07)	95(1)	0.90
111	3.37(0.26)	93(2)	3.76(0.09)	93(1)	3.32(0.06)	93(1)	2.78(0.08)	93(1)	0.86
137	–	–	2.53(0.32)	106(4)	2.03(0.18)	114(3)	1.51(0.29)	111(6)	0.00
161	–	–	2.00(0.21)	104(3)	1.94(0.17)	110(2)	1.81(0.29)	103(5)	0.48

respectively. The position angles in the equatorial coordinate system are measured from the north increasing eastward. Columns 10 and 11 represent $E(B - V)$ (Joshi & Sagar 1983) and the membership probabilities (M_P) (Stone 1977; Joshi & Sagar 1983; Huestamendia, del Rio & Mermilliod 1993), respectively. Stars with $M_P \geq 0.70$ are considered as cluster members in this study.

In Table 3, we present previous polarization measurements of stars in the direction of NGC 645 carried out by Samson (1976) and Pandey et al. (2005). Samson (1976) observed 14 stars in the direction of NGC 654 using plates with IIa0 emulsion. The IIa0 emulsion has a red cut-off similar to Johnson B band. The limiting magnitude was $B = 15$ mag. In column 1, we give the identification numbers which are adopted from Samson (1976) and Pandey et al. (2005). Columns 2–9 give P per cent and θ in B, V, R and I filters, respectively. The errors of measurements are given in parenthesis wherever available. Samson (1976) gives polarization in magnitudes (p). We converted p to P per cent using the relation P per cent $= 46.05p$ (Whittet 1992). The position angles given by Samson (1976) are with respect to the east, as deduced from the star #54. We transformed the values to with respect to the north. In column 10 we give the membership probabilities of stars obtained from Stone (1977).

The sky projection of the V-band polarization vectors for the 61 stars observed by us in NGC 654 are shown in Fig. 1 [R-band image is reproduced from the Digitized Sky Survey (DSS)]. The polarization vectors are drawn with the observed stars at the centre. The length of the polarization vector is proportional to the percentage of polarization in V band (P_V) and it is oriented parallel to the direction of corresponding observed polarization position angle in V band (θ_V). The dashed line represents the Galactic parallel at $b = -0°.52$ inclined at $\sim 100°$ with respect to the north. The stars with

$M_P \geq 0.70$ are identified using closed star symbols in green. Polarization vectors for seven stars observed by Pandey et al. (2005) are also shown in blue. Clearly, there exist stars with vectors (i) distributed about the Galactic plane and (ii) slightly greater than the Galactic plane (especially those located to the west and to the south-western regions of the cluster). This indicates that the dust grains along the lines of sight are mostly aligned by a magnetic field which is nearly parallel to the direction of the Galactic disc. But a second component of magnetic field which is slightly inclined to the Galactic disc could also be present along the lines of sight of stars showing steeper angles.

In Fig. 2 we present the sky projection of the B-band polarization vectors for the 61 stars observed by us in NGC 654 (vectors in black) along with the results from Samson (1976) (in red) and Pandey et al. (2005) (in blue). There are a few stars in common among the three observations. The star #35, identified with BD+61 315, from our list is the same as the star #64 of Samson (1976) and the star #68 of Pandey et al. (2005). While the P per cent measurements are found to be in agreement among all the three observations within the uncertainty, the θ_B of Pandey et al. (2005) seems to be 85°, 14° less than the value (99°) obtained both in our measurements and by Samson (1976). A faint reflection nebulosity (Kutner et al. 1980; Magakian 2003) is found to be associated with BD+61 315. We suspect that, due to the lack of grid in our polarimeter, the reflection nebulosity may have contributed polarized light over the aperture used for the photometry. But, since the nebulosity is faint and no stars are located along the north–south except one close to BD+61 315 (within 1 arcsec), we confidently believe that none of the other stars got affected by this nebulosity. In addition to this, two other stars from our list, stars #34 and #39, are the same as stars #56 and #66, respectively, in Samson (1976). Both of them showed
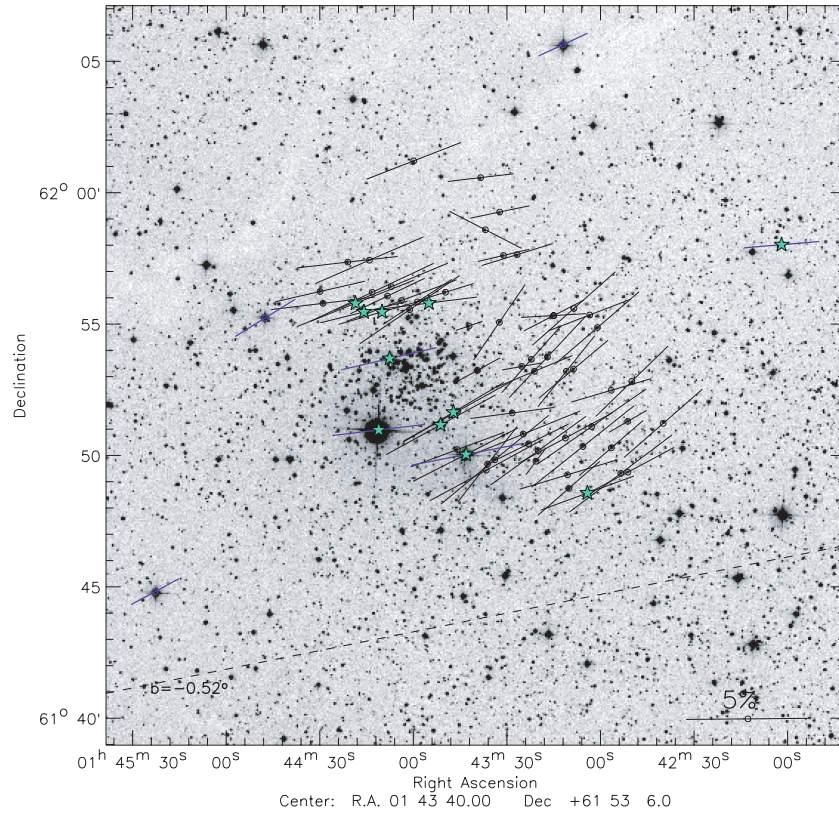
Figure 1. The 28×28 arcmin^2 *R*-band DSS image of the field containing NGC 654, reproduced from DSS. The position angles, in the equatorial coordinate system, are measured from the north, increasing eastward. The polarization vectors are drawn with the star as the centre. Length of the polarization vector is proportional to the percentage of polarization P_V and it is oriented parallel to the direction corresponding to the observed polarization position angle θ_V. A vector with a P of 5 per cent is shown for reference. The dashed line represents the Galactic parallel at $b = -0°.52$. Stars with $M_P \geq 0.70$ are identified with closed star symbols in green. Polarization vectors of seven stars observed by Pandey et al. (2005) are shown in blue.

significant differences in their P per cent and θ_B when compared. The star #66 from Samson (1976) showed the highest polarization detected in this direction ($\sim 14 \pm 0.5$ per cent). Inspection of another star, #1, in Samson (1976) which is same as the star #111 in Pandey et al. (2005) showed a difference of ~ 1 per cent polarization though θ_B seems to be consistent within uncertainty.

In Fig. 3, we compare our results with those obtained by Samson (1976) and Pandey et al. (2005) using a P_B versus θ_B plot. Our results are represented by filled black circles and those of Samson (1976) and Pandey et al. (2005) are shown using filled red circles and blue squares, respectively. The results for stars observed by us are, in general, consistent with those observed by Pandey et al. (2005). But the P_B obtained by Samson (1976) show systematically higher values (as high as ~ 14 per cent) than those obtained in both our observations and those of Pandey et al. (2005).

We used the Heiles (2000) catalogue which has a compilation of over 9000 polarization measurements to determine whether the observed polarization of stars towards the NGC 654 by us are consistent with those available in the catalogue towards the same direction. For this, we searched the catalogue for stars with polarization measurements within a circular region of radius $2°$ around NGC 654. We found 75 stars with polarization measurements in the V band. We could not show them in Fig. 1 because the nearest of them was at ~ 17 arcmin ($01^h 46^m 03^s$, $+62°01'03''$) away from NGC 654 ($01^h 44^m 00^s$, $+61°53'06''$). In the upper panel of Fig. 4, we show P_V versus θ_V plot. Our results are represented by filled black circles. The results from Pandey et al. (2005) and Heiles (2000) are

represented by filled green circles and blue squares. The stars with $M_P \geq 0.70$ are identified using open circles.

The P_V of the stars observed by us are found to be in the range of ~ 1 to ~ 5 per cent. The mean value of P_V and θ_V are found to be 3.5 ± 1 per cent and $\sim 104° \pm 9°$, respectively. The stars from Heiles (2000) show degree of polarization (P_H) in the range from ~ 0.2 to ~ 6 per cent. The mean value of P_H and position angle are $\sim 3 \pm 1.7$ per cent and $\sim 102° \pm 9°$, respectively. The range in degree of polarization and position angles obtained by us for a smaller region ($\sim 25 \times 25$ arcmin^2) are similar to those for a larger region from Heiles (2000) implying that the cause of polarization is possibly due to dust grains distributed in an extended structure and therefore likely to be located closer to the Sun than the cluster. A number of stars selected from Heiles (2000) show a higher degree of polarization ($\gtrsim 5$ per cent) and among them, five stars are located towards the direction of NGC 663 which is found to be at a distance of ~ 2 kpc (Kharchenko et al. 2005) similar to NGC 654. Thus stars in this direction can show a degree of polarization as high as ~ 6 per cent but certainly not ~ 14 per cent, as obtained by Samson (1976). It is possible that stars which showed high polarization in Samson (1976) could be unique and definitely require further multiwavelength investigations. Eight out of 11 stars with $M_P \geq 0.70$ are found to be clustering towards position angles which are lower than the mean value of $104°$.

In the lower panel of Fig. 4, we show the distribution of V-band position angles for stars from our observations. The distribution is strongly peaked but shows a significant high position angle 'tail'. A
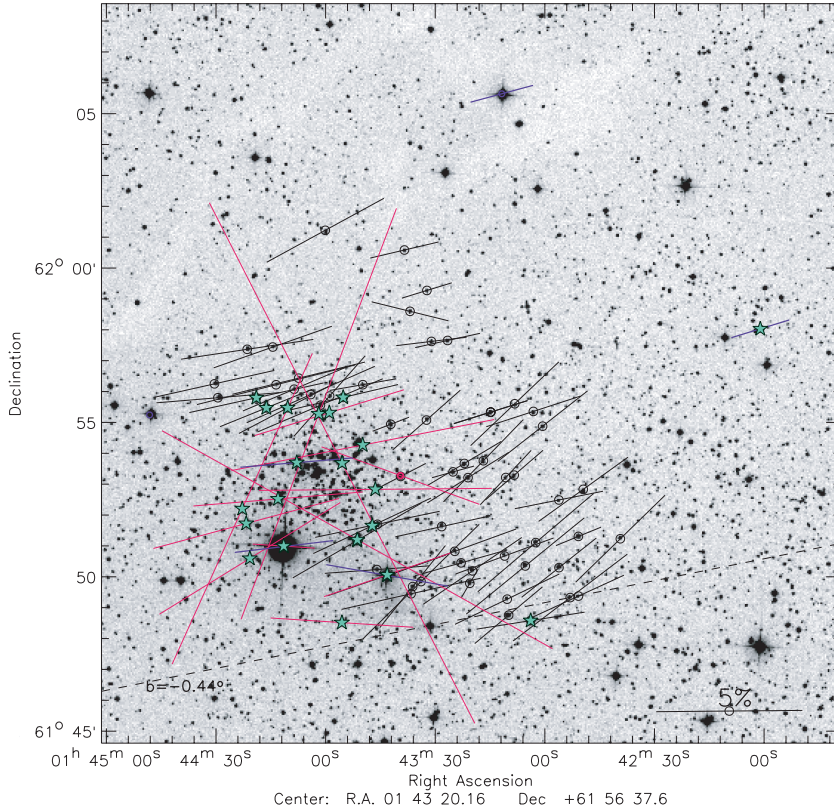
Figure 2. Same as in Fig. 1 but for P_B and θ_B. Results for 14 stars observed by Samson (1976) using IIa0 emulsion plates (which has a red cut-off similar to the Johnson *B* band) are shown using vectors drawn in red. Three out of five stars for which Pandey et al. (2005) had *B*-band measurements are also shown using vectors in blue.

Gaussian fit to the distribution is shown with peak value occurring at 102° with a dispersion in position angle of 7°. The dispersion in position angle is found to be lower in NGC 654 when compared to those for NGC 6204 and 6193 (15°1 and 16°, respectively; Waldhausen, Martínez & Feinstein 1999) and similar to those for NGC 6611 (9°3, Bastien et al. 2004), NGC 6167 (9°9, Waldhausen et al. 1999), Stock 16 (6°7, Feinstein et al. 2003) and IC 1805 (6°5, Medhi et al. 2007). Presence of a tail in the distribution of position angles towards other clusters (e.g. NGC 6167, Waldhausen et al. 1999) were attributed to the dust layers located foreground to those clusters. In Figs 1 and 2 we noted presence of opaque patches to the north of the cluster. Therefore to interpret the polarimetric results, it is important to understand the distribution of interstellar dust towards the direction of NGC 654.

### 3.1 Distribution of interstellar matter in the region of NGC 654

Samson (1975) noted that $E(B - V)$ for the stars in the central area of NGC 654 were lower than the stars located near the edges of the cluster. The radial increase in $E(B - V)$ was also noted by Pandey et al. (2005). Samson (1975) proposed the following three possibilities to explain the decrease of $E(B - V)$: (i) the inner stars are predominantly cluster members and lie closer to us than the outer ones, (ii) a ring of obscuration lies between us and the cluster, and (iii) the cluster is embedded in a shell of dust whose inner surface has a 3.6-arcmin diameter. He discarded the first possibility because of the knowledge of distance modulus to inner and outer stars. The second one was discarded on the basis of the statistical

argument that it is unlikely that such a ring of obscuration would lie exactly between us and NGC 654, and he thus favoured the third possibility of a shell around NGC 645.

Dobashi et al. (2005) recently produced extinction maps of the entire region of the Galaxy in the galactic latitude range $|b| \lesssim 40°$ using the optical data base 'Digitized Sky Survey I' and applying traditional star count technique. We obtained the fits, images of the extinction map of the field containing NGC 654 from their online website.[1] In Fig. 5 we present the high-resolution extinction map overlaid with *V*-band results from our observations and from Pandey et al. (2005) using vectors drawn in green and blue, respectively. Fig. 6 is same as Fig. 5 but is overlaid with *B*-band results from this paper, Pandey et al. (2005) and Samson (1976). Because the A_V maps shown are in galactic coordinates, we transformed all position angles measured relative to the equatorial north to the Galactic north using the relation given by Corradi, Aznar & Mampaso (1998). The square in blue identifies the centre of the cluster ($l = 129°08$, $b = -0°36$). The colour bar on the right-hand side shows the range of A_V values in figures. The contours are plotted at $A_V = 0.5$ to 2.9 with an interval of 0.3 mag.

The extinction towards the location of the cluster (blue square) shows relatively low ($A_V < 1$) values. But the outer regions of the cluster especially towards the north and the east, the extinction increases up to ∼3 mag. Two clumps identified by Dobashi et al. (2005) in these regions are labelled as P1 and P2 in Figs 5 and 6. Three dark clouds, LDN 1332, LDN 1334 and LDN 1337, identified

---

[1] http://darkclouds.u-gakugei.ac.jp/astronomer/astronomer.html.
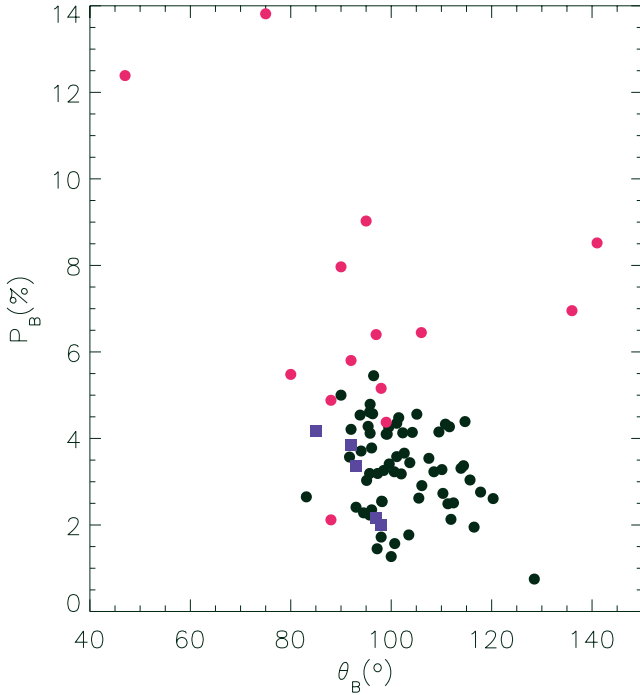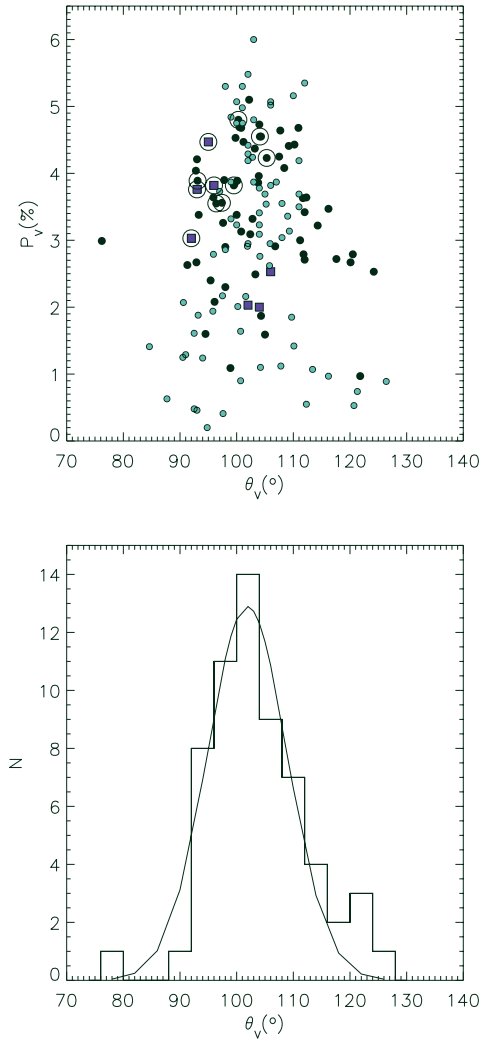
Figure 3. The P_B versus θ_B plot for 61 stars observed by us in the direction of NGC 654 are shown using black filled circles. Results of stars observed by Samson (1976) and Pandey et al. (2005) are shown using filled red circles and blue squares.

Figure 4. Upper panel: the P_V versus θ_V plot for 61 stars observed by us in the direction of NGC 654 are shown using black filled circles. Results of stars observed by Heiles (2000) and Pandey et al. (2005) are shown using filled green circles and blue squares. The stars with $M_P \geq 0.70$ are identified using open circles. Lower panel: distribution of *V*-band position angles for the stars from our observations.

towards the direction of NGC 654 are located close to P1 and P2. While LDN 1332 and LDN 1334 are found to be radially 4 and 7 arcmin, respectively, away from the clump P1, LDN 1337 is found to be radially 11 arcmin away from the clump P2. Note that the A_V values estimated in the extinction map towards the centre of the cluster are less than the values estimated by Samson (1976) and Pandey et al. (2005) by a factor of ∼3. This could be because of the coarse resolution of the extinction map of Dobashi et al. (2005) and the values could be averages.

It is interesting to note that the overall morphology of the dust distribution in this region resembles a ring structure with a central hole coinciding with the position of the cluster. Structurally the distribution is highly inhomogeneous. This ring morphology of dust distribution explains the increase in $E(B - V)$ values found by Samson (1975) and Pandey et al. (2005) towards the edges or outer parts of the cluster. Therefore the second possibility proposed by Samson (1976), which he discarded on statistical grounds, arguing that it is unlikely that a ring of obscuration would lie exactly between us and NGC 654, seems to be the most plausible scenario. We rule out the third possibility proposed by Samson (1976), i.e. the cluster being embedded in a shell of dust because, using the star count method, it would be difficult to detect dust obscuration located at ∼2 kpc since the cloud would become inconspicuous due to the large number of foreground stars.

In order to determine distances to the foreground dust concentrations, we obtained distances and $E(B - V)$ of main-sequence stars located within a circle of radius 1° around NGC 654 from the catalogue 'Interstellar Matter in the Galactic Disc' produced by Guarinos (1992). In Fig. 7, we show the $E(B - V)$ versus distance (pc) plot. The plot shows $E(B - V)$ increasing sharply at two distances, ∼240 pc and ∼1 kpc, indicating that there could be at least two layers of dust, one at ∼240 pc and another at ∼1 kpc, in the

direction of NGC 654. Using star counts and counts of extragalactic nebulae, Heeschen (1951) also showed the presence of obscuring material at ∼200–300 pc and at ∼800 pc. The obscuring material located at ∼240 pc contributes an $E(B - V) \sim 0.5$ mag while net colour excess produced at 1 kpc is found to be ∼0.85 mag. The stars with $M_P \geq 0.70$ are identified using open circles. These stars are assumed to be at a distance of 2.4 kpc. From the figure it is evident that the extinction suffered by the cluster members of ≥0.69 mag are mainly due to the dust layers present within 1 kpc from us.

In their photometric study of 23 open clusters, Phelps & Janes (1994) pointed out that the colour–magnitude diagram of NGC 654 showed lack of the characteristic wedge-shaped distribution of the field stars. The cluster being located in front of a cloud is suggested to be the cause (Phelps & Janes 1994). The presence of a reflection nebulosity (Kutner et al. 1980; Magakian 2003) associated with BD+61 315 (star #555, $M_P = 0.84$) shows that the cluster is indeed associated with a cloud. But, the relatively low $E(B - V) = 0.88$ of this star, similar to the $E(B - V)$ of 0.85 mag
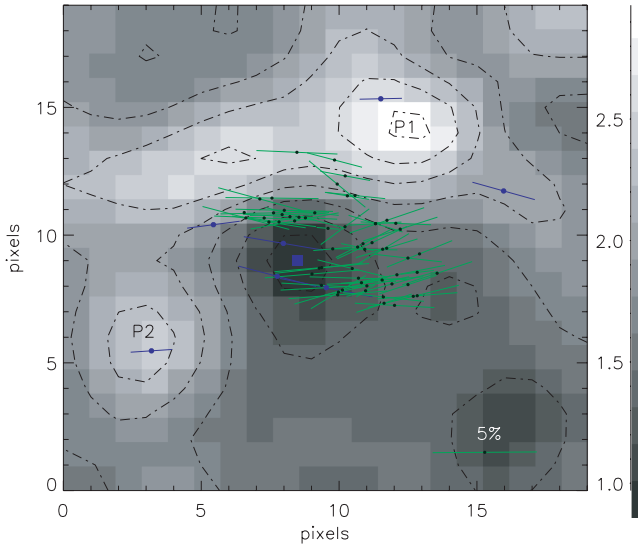
Figure 5. The high-resolution extinction map of the region (30 × 30 arcmin^2) produced by Dobashi et al. (2005) using the optical data base 'Digitized Sky Survey I' and applying the traditional star count technique. We overlay *V*-band results from our observations and from Pandey et al. (2005) using vectors drawn in green and blue, respectively. Colour schemes are made different from previous figures for more clarity. The two clumps identified by Dobashi et al. (2005) in this region are identified and labelled as P1 and P2. The centre of the cluster ($l = 129°08$, $b = −0°36$) is identified using blue square.
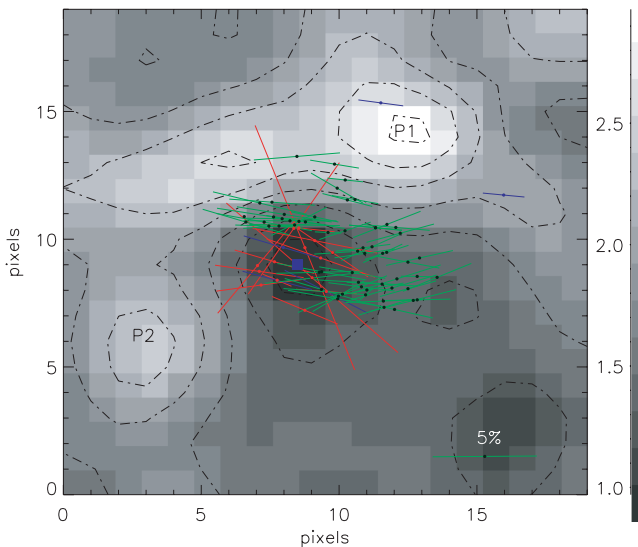
Figure 6. Same as the Fig. 5 but we overlay with *B*-band results from this paper, Pandey et al. (2005) and Samson (1976). The vectors shown in red are the results from Samson (1976).

produced by obscuring material located at ∼200–1 kpc (Fig. 7), suggests that the star (also the cluster) is located just in front of the associated cloud. This is further supported by the results of Pandey et al. (2005) that at the centre of the cluster $E(B − V) < 1$ mag. This further strengthens the argument that the extinction towards the cluster is mainly contributed by the material distributed within 1 kpc from us. Because there is a cloud behind the cluster, the stars including those with higher membership probability observed by us may not be behind the cloud behind the cluster. Henceforth, we
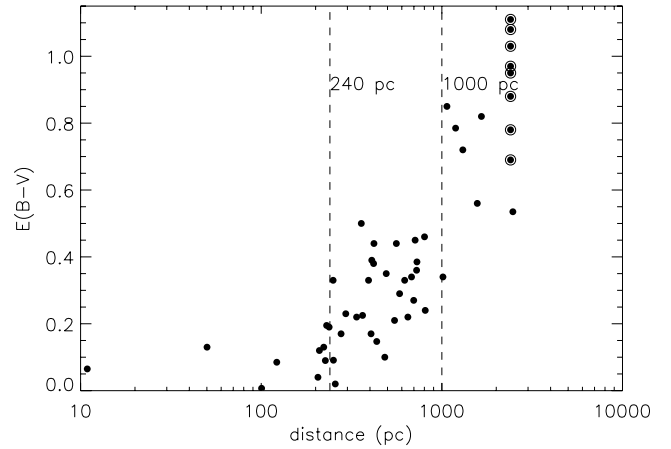
Figure 7. The distances of stars are plotted against their $E(B − V)$ from the data obtained from Guarinos (1992). The stars with $M_P \geq 0.70$ are identified using open circles. These stars are assumed to be at a distance of 2.4 kpc. The dotted lines are drawn at 240 and 1000 pc to show a sharp increase in $E(B − V)$ value at these distances.

believe that the observed polarization towards NGC 654 is due to the aligned dust grains associated with the clouds located at ∼200 and ∼800–1000 pc.
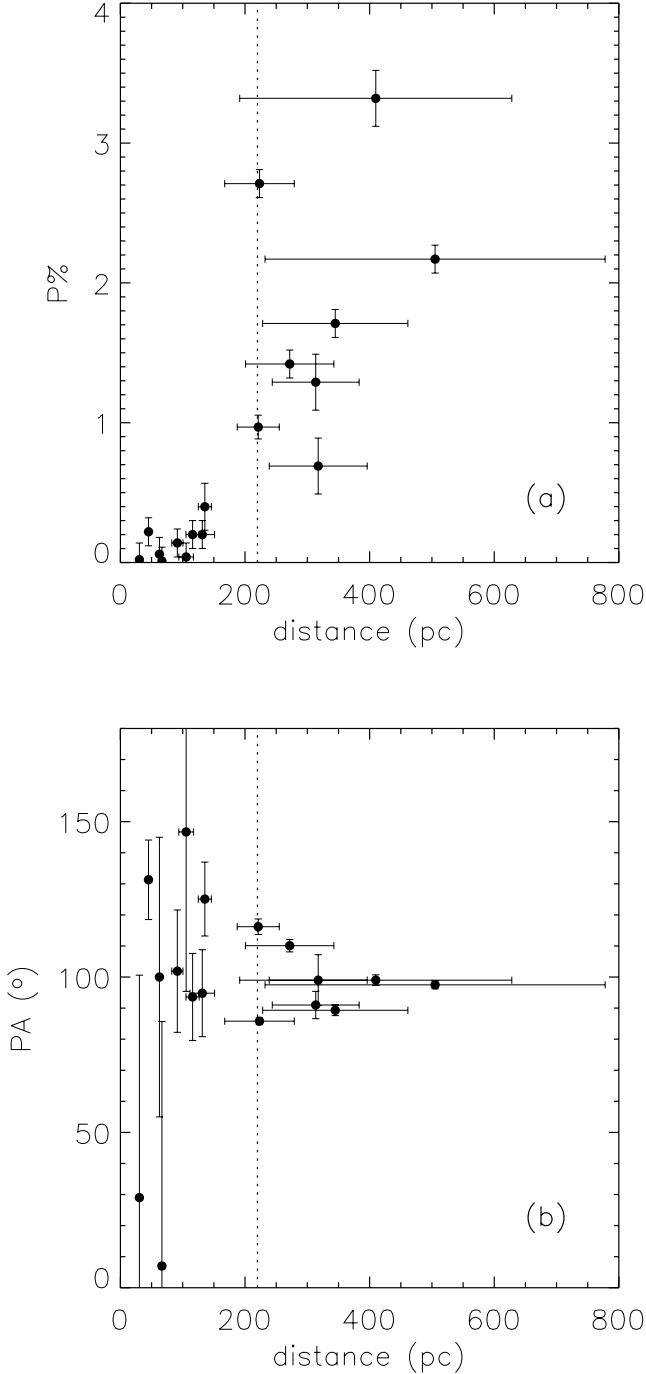
In order to investigate the polarization properties of dust grains located at different distances from us, we selected all the stars from within a circle of radius 3° around NGC 654 for which polarization and parallax measurements are available in Heiles (2000) and the *Hipparcos*, respectively. The *Hipparcos* parallax measurements are obtained from the *Hipparcos* and *Tycho* Catalogues (Perryman et al. 1997 and Høg et al. 1997). We did not include the stars observed by us because of the lack of distance information for them except for the cluster member stars. Stars which showed peculiar features and emissions in their spectrum, as given by SIMBAD, are rejected.

In Figs 8(a) and (b) we present the degree of polarization (P_{hip}) and position angle (θ_{hip}) versus distance plots, respectively. As expected, stars located closer to us show low P_{hip} ($\lesssim 0.5$ per cent) with a large scatter in their θ_{hip}. Stars located beyond ∼220 pc showed relatively high values of P_{hip} in the range from 1 to 3.3 per cent with a sharp jump in polarization (≥ 1 per cent) occurring at ∼220 pc. But there are no stars between ∼150 and ∼200 pc, so we can only infer a maximum distance to the dust grains responsible for the observed sharp jump from Fig. 8. However, since the abrupt increase in both $E(B − V)$ (Fig. 7) and P_{hip} (Fig. 8) are found to occur at 220–240 pc, we assign a maximum distance of 220 pc to the first layer.

Among the two stars which showed a sharp jump in P_{hip} at ∼220 pc, the one with higher P_{hip} (2.7 per cent) shows a θ_{hip} of $86° \pm 1°$ and the other with lower P_{hip} (1 per cent) shows a θ_{hip} of $116° \pm 3°$. Beyond ∼220 pc, the P_{hip} increases with the distance of the stars and θ_{hip} shows less scatter as it tends to become more parallel to the Galactic plane. This implies that though the majority of the dust grains in the direction of NGC 654 are aligned parallel to the Galactic plane, there are two additional populations of dust grains located in the first layer at ∼220 pc which are responsible for producing polarization with position angles both less than and greater than the Galactic parallel.

If the polarization of the starlight is caused due to the alignment of dust grains with the local magnetic field, then this implies that

3.2 Serkowski law

The maximum wavelength (λ_{max}) and the maximum polarization (P_{max}) are both functions of the optical properties and characteristic of particle size distribution of the aligned dust grains (McMillan 1978; Wilking et al. 1980). Moreover, it is also related to the interstellar extinction law (Serkowski et al. 1975; Whittet & van Breda 1978; Coyne & Magalhaes 1979; Clayton & Cardelli 1988). The λ_{max} and P_{max} have been calculated by fitting the observed polarization in the B, V and R bandpasses to the standard Serkowski's polarization law:

$$P_\lambda / P_{max} = \exp[-\,k \ln^2 (\lambda_{max}/\lambda)] \qquad (1)$$

and adopting the parameter $k = 1.15$ (Serkowski 1973). In the fits the degree of freedom adopted is 1. Though there are only three data points, the wavelength covered ranges from 0.44 to 0.66 µm and all the λ_{max} found fell within this range. Since we have enough wavelength coverage, the fit is reasonably fine but sometimes it may cause one to overestimate the value of σ_1. We computed the σ_1 parameter (the unit weight error of the fit) for each star. If the polarization is well represented by the Serkowski's interstellar polarization law, σ_1 should not be higher than 1.6 due to the weighting scheme. A higher value could be indicative of the presence of intrinsic polarization. The λ_{max} can also give us a clue about the origin of polarization. The stars which have λ_{max} lower than the average value of the ISM (0.55 ± 0.04 µm; Serkowski et al. 1975) are the probable candidates to have an intrinsic component of polarization (Orsatti, Vega & Marraco 1998). The dispersion of the position angle ($\bar{\epsilon}$) for each star normalized by the mean value of the position angle errors is another tool to detect the intrinsic polarization. The values obtained for P_{max}, σ_1, λ_{max} and $\bar{\epsilon}$ together with RA (J2000) and Dec. (J2000) for all the 61 observed stars with their respective errors are given in Table 4.

Out of 61 observed stars, three non-member stars (viz. #16, #24 and #50) and one member star (viz. #39) have the σ_1 value above the limit of 1.6. Dispersion in position angle $\bar{\epsilon}$ is higher for the member star #12 and non-member stars #22, #24, #30 and #50. Out of these above-mentioned seven probable candidates detected by using two criteria σ_1 and $\bar{\epsilon}$, the value of λ_{max} is smaller than the normal size of the grains only for the member star #12 and non-member star #16. Although the non-member star #16 is found to have a higher value of σ_1 and lower value of λ_{max}, $\bar{\epsilon}$ is found to be very small. In the case of star #12, the value of $\bar{\epsilon}$ is high, which indicates a rotation in position angle and implies that the polarization is produced by a combination of different dust populations. Nevertheless, in majority of the observed stars, the polarization is found to be caused due to the foreground dust grains.

The weighted mean of λ_{max} for the member and non-member stars are obtained as 0.52 ± 0.01 µm and 0.54 ± 0.01 µm, respectively. There is not much difference in the weighted mean of λ_{max} between the member and the non-member stars of NGC 654, which implies that the lights from the both member and non-member stars encountering the same population of foreground dust grains. Moreover, these values are very close to the mean interstellar value of λ_{max} 0.55 ± 0.04 µm. Therefore, we can also conclude that the characteristic grain size distribution as indicated by the polarization study of stars in NGC 654 is nearly the same as that for the general ISM. The weighted mean of the maximum polarization for the member stars and non-member stars obtained are 3.74 ± 0.01 and 2.87 ± 0.01 per cent, respectively.

Figure 8. (a) The polarization as a function of distance is plotted. The distances are estimated from *Hipparcos* parallax measurements and P per cent values are from Heiles (2000) catalogue. (b) Position angles are plotted for the same set of stars as a function of their distances.

there exist two components of the magnetic field which are responsible for the observed polarization properties. While the magnetic field component aligned more parallel with the Galactic plane is dominant towards high extinction regions, the magnetic field component which is found to be steeper than the Galactic parallel seems to be dominant towards the west and the south-west regions of NGC 654.

Table 4. The $P_{max}, \lambda_{max}, \sigma_1$ and $\bar{\epsilon}$ for the observed data in NGC 654.

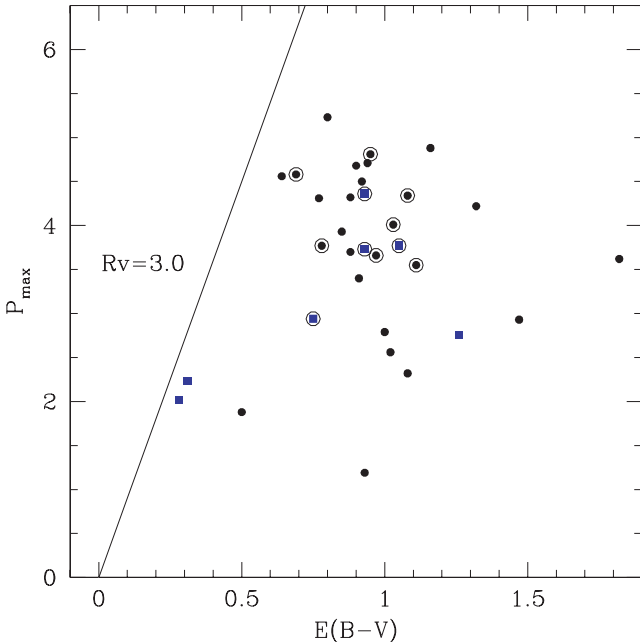| Serial No.	RA (2000J)	Dec. (2000J)	$P_{max} \pm \epsilon$ (per cent)	σ_1	$\lambda_{max} \pm \epsilon$ (μm)	$\bar{\epsilon}$
01	01 42 39.54	61 51 18.4	3.50 ± 0.08	0.43	0.58 ± 0.05	0.81
02	01 42 49.68	61 52 50.9	3.22 ± 0.02	0.83	0.56 ± 0.05	1.32
03	01 42 51.02	61 51 19.4	1.62 ± 0.01	0.74	0.54 ± 0.03	0.92
04	01 42 51.00	61 49 23.4	3.49 ± 0.15	1.55	0.57 ± 0.05	0.56
05	01 42 53.27	61 49 20.5	4.41 ± 0.13	0.20	0.53 ± 0.02	0.44
06	01 42 56.33	61 50 18.7	2.81 ± 0.05	0.93	0.48 ± 0.02	1.06
07	01 42 56.36	61 52 30.2	3.23 ± 0.01	0.08	0.55 ± 0.01	0.66
08	01 43 00.81	61 55 00.8	3.63 ± 0.01	0.42	0.55 ± 0.01	0.58
09	01 43 03.34	61 55 29.5	3.44 ± 0.05	0.26	0.57 ± 0.03	0.22
10	01 43 08.45	61 55 44.4	3.71 ± 0.07	0.15	0.61 ± 0.03	0.21
11	01 43 02.69	61 51 07.4	4.74 ± 0.12	0.25	0.60 ± 0.01	2.21
12	01 43 04.08	61 48 35.7	3.77 ± 0.03	0.59	0.49 ± 0.01	4.35
13	01 43 05.56	61 50 21.9	4.45 ± 0.11	0.29	0.51 ± 0.01	1.78
14	01 43 10.11	61 48 46.3	2.57 ± 0.04	0.86	0.51 ± 0.02	0.33
15	01 43 10.51	61 49 17.4	3.79 ± 0.05	0.22	0.51 ± 0.02	0.64
16	01 43 11.22	61 50 41.3	3.93 ± 0.24	2.14	0.49 ± 0.05	1.09
17	01 43 08.59	61 53 18.5	2.39 ± 0.02	1.46	0.52 ± 0.13	0.28
18	01 43 10.91	61 53 13.8	2.42 ± 0.03	0.95	0.52 ± 0.12	0.72
19	01 43 15.02	61 55 28.1	2.57 ± 0.03	0.28	0.50 ± 0.01	1.20
20	01 43 15.03	61 55 28.2	2.64 ± 0.01	0.03	0.52 ± 0.01	1.63
21	01 43 17.03	61 53 46.4	3.22 ± 0.11	1.09	0.55 ± 0.04	2.01
22	01 43 21.23	61 53 13.6	3.13 ± 0.01	0.71	0.54 ± 0.01	4.63
23	01 43 22.23	61 53 41.2	2.76 ± 0.04	0.27	0.56 ± 0.02	1.68
24	01 43 25.32	61 53 24.8	1.57 ± 0.01	2.29	0.57 ± 0.05	3.23
25	01 43 20.00	61 50 12.4	3.79 ± 0.27	1.11	0.50 ± 0.06	0.26
26	01 43 20.74	61 49 48.3	0.82 ± 0.05	0.78	0.58 ± 0.05	0.84
27	01 43 23.13	61 50 28.0	3.33 ± 0.01	0.04	0.54 ± 0.01	1.77
28	01 43 24.85	61 50 50.4	4.45 ± 0.19	0.36	0.54 ± 0.05	0.45
29	01 43 32.36	61 55 12.7	2.56 ± 0.01	0.05	0.50 ± 0.01	1.15
30	01 43 28.43	61 51 38.5	3.40 ± 0.01	0.49	0.56 ± 0.01	3.49
31	01 43 34.08	61 49 51.6	4.50 ± 0.16	0.89	0.51 ± 0.02	2.00
32	01 43 36.39	61 49 41.9	2.79 ± 0.01	0.13	0.54 ± 0.01	0.15
33	01 43 36.81	61 49 27.9	4.88 ± 0.12	0.94	0.57 ± 0.04	1.80
34	01 43 39.68	61 53 15.9	1.88 ± 0.01	1.53	0.56 ± 0.01	1.56
35	01 43 43.51	61 50 03.5	4.32 ± 0.05	0.64	0.54 ± 0.02	1.42
36	01 43 46.18	61 50 14.9	3.62 ± 0.12	1.26	0.48 ± 0.03	2.17
37	01 43 46.03	61 51 42.9	4.56 ± 0.15	0.48	0.53 ± 0.02	2.70
38	01 43 47.45	61 51 40.1	4.34 ± 0.04	1.41	0.55 ± 0.08	0.66
39	01 43 51.62	61 51 11.3	4.58 ± 0.05	1.78	0.53 ± 0.01	1.13
40	01 43 26.83	61 57 40.2	2.84 ± 0.13	1.46	0.48 ± 0.10	0.36
41	01 43 31.24	61 57 38.3	2.41 ± 0.15	0.98	0.53 ± 0.07	0.67
42	01 43 37.10	61 58 36.8	2.83 ± 0.28	0.74	0.47 ± 0.06	1.46
43	01 43 32.48	61 59 17.4	2.06 ± 0.08	0.71	0.62 ± 0.09	0.23
44	01 43 38.64	62 00 36.0	2.65 ± 0.04	0.30	0.55 ± 0.03	0.65
45	01 43 42.38	61 54 57.3	1.19 ± 0.08	1.17	0.55 ± 0.01	0.93
46	01 43 50.02	61 56 14.3	2.32 ± 0.04	0.52	0.49 ± 0.02	1.00
47	01 43 55.40	61 55 49.5	4.01 ± 0.05	0.51	0.56 ± 0.07	0.57
48	01 43 59.12	61 55 52.2	2.93 ± 0.07	0.40	0.49 ± 0.03	1.68
49	01 44 00.30	62 01 14.3	4.11 ± 0.15	0.58	0.49 ± 0.04	0.84
50	01 44 01.63	61 55 34.3	4.31 ± 0.05	2.46	0.59 ± 0.03	4.16
51	01 44 04.29	61 55 55.1	4.68 ± 0.11	0.78	0.53 ± 0.01	1.66
52	01 44 07.58	61 56 26.9	4.71 ± 0.01	0.02	0.52 ± 0.01	1.84
53	01 44 08.81	61 56 05.5	3.70 ± 0.10	1.27	0.53 ± 0.03	1.32
54	01 44 10.59	61 55 29.3	3.66 ± 0.01	0.17	0.57 ± 0.07	0.97
55	01 44 13.77	61 56 14.1	5.23 ± 0.17	0.88	0.50 ± 0.03	0.71
56	01 44 14.67	61 57 27.4	4.28 ± 0.08	0.20	0.52 ± 0.02	0.16
57	01 44 16.44	61 55 29.1	3.55 ± 0.02	0.08	0.58 ± 0.08	0.35
58	01 44 19.17	61 55 48.8	4.81 ± 0.06	0.05	0.53 ± 0.01	0.96
59	01 44 21.67	61 57 23.0	4.29 ± 0.27	1.42	0.53 ± 0.08	0.33
60	01 44 29.70	61 55 48.9	4.22 ± 0.04	1.14	0.53 ± 0.04	0.43
61	01 44 30.64	61 56 15.9	3.93 ± 0.26	1.04	0.53 ± 0.07	0.87

3.3 Polarization efficiency

For interstellar dust particles in diffuse ISM the ratio between the maximum amount of polarization and visual extinction (polarization efficiency) cannot exceed the empirical upper limit (Hiltner 1956)

$$P_{max} < 3A_V \simeq 3R_V E(B-V). \tag{2}$$

The ratio $P_{max}/E(B-V)$ mainly depends on the alignment efficiency, magnetic strength and the amount of depolarization due to radiation traversing more than one cloud in different directions.

Fig. 9 shows the relation between colour excess $E(B-V)$ and maximum polarization P_{max} for the stars observed by us (black filled circle) and Pandey et al. (2005) (blue filled square) towards NGC 654 produced by the dust grains along the line of sight to the cluster. Colour excess $E(B-V)$ is taken from the work of Joshi & Sagar (1983) and Huestamendia et al. (1993). Among the 61 stars observed by us $E(B-V)$ is available for only 26 stars (eight member and 18 non-member). In the efficiency diagram none of the stars are lying to the left-hand side of the interstellar maximum line. In the previous section, though we suspect two member stars, #12 and #39, as candidates for intrinsic polarization by using different criterion, they also fall to the left-hand side in the polarization efficiency diagram. From the polarization efficiency diagram it appears that apparently the stars are not affected by intrinsic polarization and the dominant mechanism of polarization for the observed member of NGC 654 is supposed to be the alignment of grains by magnetic field, like general ISM. This diagram also indicates that while the colour excess of the member stars of NGC 654 varies from 0.69 to 1.11 mag approximately, the variation in the polarization value is high; ~1.87 per cent. This high variation of P_{max} indicates the different populations of dust grains present in the line of sight towards NGC 654, as inferred from Section 3.1.

In Fig. 10, we plot the $P_{max}/E(B-V)$ versus $E(B-V)$ for the stars observed by us and Pandey et al. (2005) with available colour
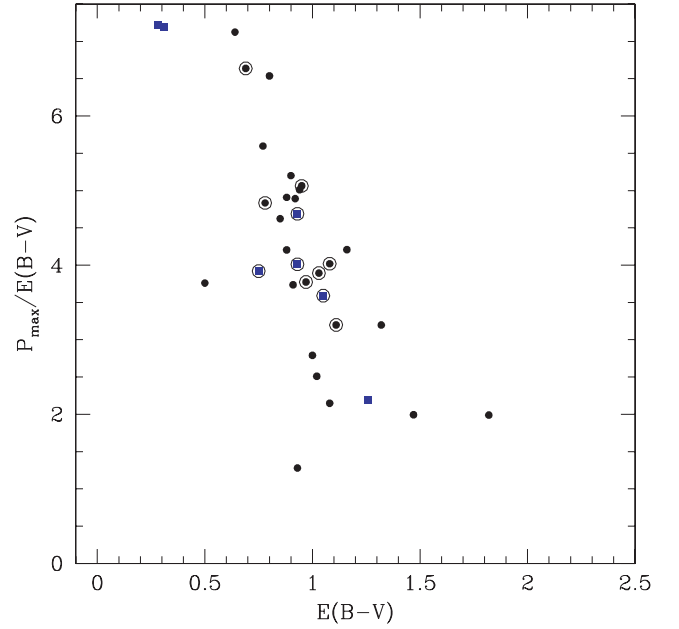
Figure 10. $P_{max}/E(B-V)$ plotted as a function of $E(B-V)$. The stars observed by us in the direction of NGC 654 are shown using black filled circles. Results of stars observed by Pandey et al. (2005) are shown using blue square. The stars with $M_P \geq 0.70$ are identified using open circles.

excess $E(B-V)$. The polarization efficiency is found to fall with the increase in $E(B-V)$. There can be two possibilities for this effect: (i) the dust grains are located in local cloud and the drop in efficiency is due to an increase in the size of the grains; (ii) the dust grains are distributed along the line of sight and the drop in efficiency is due to a slight change in the polarization position angle.

4 SUMMARY

We have observed the linear polarization for 61 stars on the region of the open cluster NGC 654. The linear polarization of the stars is caused by the foreground dust grains. Combining our results with those from the literature and various surveys, we present evidence for the presence of at least two dust layers along the line of sight to the cluster. Their distances are estimated to be ~200 pc and ~1 kpc. Both dust layers have their local magnetic field aligned roughly parallel to the Galactic plane. From the available extinction maps, we show that the dust towards NGC 654 is distributed in a ring geometry with a hole which coincides with the centre of the cluster. This explains for an increase in the extinction towards outer parts of the cluster inferred in previous studies of the region.

The weighted means of maximum polarization P_{max} for member and non-member stars are obtained as 3.74 ± 0.01 and 2.87 ± 0.01 per cent, respectively. The weighted means of maximum wavelength λ_{max} for the cluster members and the field stars are found to be 0.52 ± 0.01 and 0.54 ± 0.01 μm, respectively. These values of λ_{max} of stars towards NGC 645 are thus similar to those of ISM $(0.55 \pm 0.04$ μm), implying that the polarization is caused mainly due to the foreground dust grains, as we have inferred for the IC 1805 cluster (Medhi et al. 2007) in a previous study.

ACKNOWLEDGMENTS

We thank the referee for his constructive remarks which led to great improvement in the clarity of the paper. This research has

Figure 9. Polarization efficiency diagram. Using $R_v = 3.0$, the line of maximum efficiency drawn. The stars observed by us in the direction of NGC 654 are shown using black filled circles. Results of stars observed by Pandey et al. (2005) are shown using blue squares. The stars with $M_P \geq 0.70$ are identified using open circles.

made use of the WEBDA data base, operated at the Institute for Astronomy of the University of Vienna; use of image from the National Science Foundation and Digital Sky Survey (DSS), which was produced at the Space Telescope Science Institute under the US Government grant NAG W-2166; use of NASA's Astrophysics Data System and use of IRAF, distributed by National Optical Astronomy Observatories, USA. BJM thanks Orchid for her support.

REFERENCES

Bastien P., Ménard F., Corporon P., Manset N., Poidevin F., Duchêne G., Monin J.-L., 2004, Ap&SS, 292, 427

Clayton G. C., Cardelli J. A., 1988, AJ, 96, 695

Corradi R. L. M., Aznar R., Mampaso A., 1998, MNRAS, 297, 617

Coyne G. V., Magalhaes A. M., 1979, AJ, 84, 1200

Davis L., Jr, Greenstein J. L., 1951, ApJ, 114, 206

Dobashi K., Uehara H., Kandori R., Sakurai T., Kaiden M., Umemoto T., Sato F., 2005, PASJ, 57, 1

Feinstein C., Baume G., Vergne M. M., Vazquez R., 2003, A&A, 409, 933

Greenberg J. M., 1968, in Middlehurst B. M., Aller L. H., eds, Nebulae and Interstellar Matter. Chicago Univ. Press, Chicago, p. 221

Guarinos J., 1992, ESO Conference and Workshop Proc. 43, Astronomy from Large Data Bases II. p. 301, ISBN 3-923524-47-1

Heeschen D. S., 1951, ApJ, 114, 132

Heiles C., 2000, AJ, 119, 923

Hiltner W. A., 1956, ApJS, 2, 389

Høg E. et al., 1997, A&A, 323, 57

Huestamendia G., del Rio G., Mermilliod J. C., 1993, A&AS, 100, 25

Joshi U. C., Sagar R., 1983, MNRAS, 202, 961

Kharchenko N. V., Piskunov A. E., Röser S., Schilbach E., Scholz R. D., 2005, A&A, 440, 403

Kutner M. L., Machnik D. E., Tucker K. D., Dickman R. L., 1980, ApJ, 237, 734

Lazarian A., Goodman A. A., Myers P. C., 1997, ApJ, 490, 273

Lyngà G., 1984, Catalogue of Open Clusters Data, 1/1S70401, Centre de Donneès Stellaires, Strasbourg

Magakian T. Yu., 2003, A&A, 399, 141

McMillan R. S., 1978, APJ, 225, 880

Medhi B. J., Maheswar G., Brijesh K., Pandey J. C., Kumar T. S., Sagar R., 2007, MNRAS, 378, 881

Orsatti A. M., Vega E., Marraco H. G., 1998, AJ, 116, 266

Pandey A. K., Upadhyay K., Ogura K., Sagar R., Mohan V., Mito H., Bhatt H. C., Bhatt B. C., 2005, MNRAS, 358, 1290

Perryman M. A. C. et al., 1997, A&A, 323, 49

Phelps R. L., Janes K. A., 1994, ApJS, 90, 31

Rautela B. S., Joshi G. C., Pandey J. C., 2004, Bull. Astron. Soc. India, 32, 159

Sagar R., Yu Q. Z., 1989, MNRAS, 240, 551

Samson W. B., 1975, Ap&SS, 34, 363

Samson W. B., 1976, Ap&SS, 44, 217

Schmidt G. D., Elston R., Lupie O. L., 1992, AJ, 104, 1563

Serkowski K., 1973, in Greenberg J. M., van de Hults H. C., eds, Proc. IAU Symp. Vol. 52, Interstellar Dust and Related Topics. Reidel, Dordrecht, p. 145

Serkowski K., Mathewson D. L., Ford V. L., 1975, ApJ, 196, 261

Stone R. C., 1977, A&A, 54, 803

Waldhausen S., Martínez R. E., Feinstein C., 1999, AJ, 117, 2882

Whittet D. C. B., 1992, Dust in the Galactic Environment. IOP Publishing, Bristol

Whittet D. C. B., van Breda I. G., 1978, A&A, 66, 57

Wilking B. A., Lebofsky M. J., Kemp J. C., Martin P. G., Rieke G. H., 1980, ApJ, 235, 905

This paper has been typeset from a TEX/LATEX file prepared by the author.